

Investigation of paracetamol degradation using LED and UV-C photo-reactors

Graziele Elisandra do Nascimento, Marcos André Soares Oliveira, Rayany Magali da Rocha Santana, Beatriz Galdino Ribeiro, Deivson Cesar Silva Sales, Joan Manuel Rodríguez-Díaz, Daniella Carla Napoleão, Mauricio Alves da Motta Sobrinho and Marta Maria Menezes Bezerra Duarte

ABSTRACT

This work investigates the efficiency of LED and UV-C photo-reactors for paracetamol degradation using advanced oxidative processes. Among the evaluated processes, photo-Fenton was the most efficient for both radiations. Degradations greater than 81% (λ 197 nm) and 91% (λ 243 nm) were obtained in the kinetic study. These degradations were also observed by means of the reduction in the peaks in both spectral scanning and high-performance liquid chromatography analysis. The good fit of the Chan and Chu kinetic model shows that the degradation reaction has pseudo-first order behavior. Toxicity tests did not indicate the inhibition of growth of *Lactuca sativa* seeds and *Escherichia coli* bacterium. However, the growth of strains of the *Salmonella enteritidis* bacterium was inhibited in all the samples, demonstrating that only this bacterium was sensitive to solutions. The proposed empirical models obtained from the 2⁴ factorial designs were able to predict paracetamol degradation. These models could, at the same levels assessed, be used to predict the percentage of degradation in studies using other organic compounds. The LED and UV-C photo-reactors were, when employing the photo-Fenton process, able to degrade paracetamol, thus highlighting the efficiency of LED radiation when its power (three times smaller) is compared to that of UV-C radiation.

Key words | advanced oxidative processes, empirical mathematical models, kinetic studies, toxicity

HIGHLIGHTS

- Proposition of empirical models for predicting the paracetamol degradation.
- Use of full factorial designs to variables study involved in the processes.
- Use of the first order kinetic model proposed by Chan and Chu to fit the experimental data.
- Evaluation of the toxicity of the solutions through the use of seeds and bacteria.

Graziele Elisandra do Nascimento
(corresponding author)

Marcos André Soares Oliveira

Rayany Magali da Rocha Santana

Beatriz Galdino Ribeiro

Daniella Carla Napoleão

Mauricio Alves da Motta Sobrinho

Marta Maria Menezes Bezerra Duarte

Departamento de Engenharia Química,
Universidade Federal de Pernambuco,
Av. Prof. Arthur de Sá, s/n, 50740-521, Recife, PE,
Brazil

E-mail: grazielen@yahoo.com.br

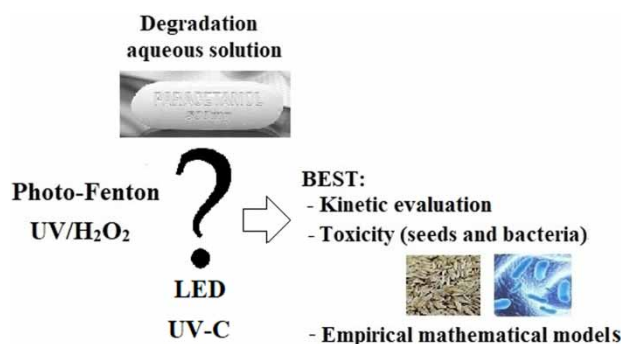
Deivson Cesar Silva Sales

Escola Politécnica de Pernambuco,
Universidade de Pernambuco,
Rua Benfica, 455, Madalena, 50720-001, Recife, PE,
Brazil

Joan Manuel Rodríguez-Díaz

Laboratorio de Análisis Químicos y
Biotecnológicos,
Instituto de Investigación, Universidad Técnica de
Manabí,
Portoviejo,
Ecuador;
Departamento de Procesos Químicos, Facultad de
Ciencias Matemáticas, Físicas y Químicas,
Universidad Técnica de Manabí,
Portoviejo,
Ecuador
and
Programa de Pós-graduação em Engenharia
Química,
Universidade Federal da Paraíba,
João Pessoa 58051-900,
Brazil

GRAPHICAL ABSTRACT



INTRODUCTION

The worldwide consumption of pharmaceutical compounds has increased noticeably in recent years (Lessa *et al.* 2018), making the detection of these compounds in the environment increasingly frequent. According to Comber *et al.* (2018), as several drugs are already being detected in surface water at different concentrations, several countries are beginning to monitor the cycle of active pharmaceutical inputs.

Water becomes polluted by pharmaceutical compounds as a result of: the inefficient treatment of effluents originating from the pharmaceutical industry and hospitals (drugs or metabolites released and excreted in patients' urine); or drugs that are released without use into the sewage system, and the use of antibiotics and hormones in cattle (Feier *et al.* 2018).

The main classes of drugs most commonly found in the environment are antibiotics, analgesics, antiepileptics, anti-psychotics, antiretrovirals and insulin analogues (Beek *et al.* 2016). One drug that is widely used as an analgesic and antipyretic for humans is Paracetamol (4-acetaminophen). This compound and its metabolites have already been found in surface water, wastewater and drinking water worldwide (Wu *et al.* 2012). Although studies indicate that the drugs are found in low concentrations in the environment, these compounds may be present in concentrations of milligrams per liter (mg·L⁻¹) in the receiving surface waters near pharmaceutical industries facilities (Serpone *et al.* 2017).

The presence of paracetamol and other drugs in the water poses a threat to health and the environment. This is owing to their toxicity, bioaccumulation in living organisms and resistance to biological degradation processes

(Feier *et al.* 2018). The damage that these compounds may cause to living organisms and the environment, along with the inadequacy of the treatment techniques applied in conventional wastewater treatment plants, have led to the study of methods that are efficient for degradation of these compounds (Prasse *et al.* 2015).

In this context, advanced oxidative processes (AOP) are consolidated to be an efficient form of treatment for persistent organic pollutants (Lee *et al.* 2016). Among the AOP, those that occur in the presence of light, the so-called photolytics, stand out due to their applicability in treating these types of pollutants. Some of these photolytic processes have already been used in the degradation of pharmaceutical products, such as photoperoxidation (UV/H₂O₂), photo-Fenton and heterogeneous photocatalysis (Lofrano *et al.* 2017; Kanakaraju *et al.* 2018; Kowalska *et al.* 2020).

The use of photolytic reactors in degradation processes by AOP offers, as advantages, the use of multiple lamps (equipped in series or in parallel), the possibility to control the power of the light sources, the desired reaction time, the present atmosphere and the application of agitation or not. In addition, it ensures that the reaction species present in the reactor completely absorb the light irradiations used during the process (Katic *et al.* 2018; Nguyen & Wu 2018; Russo *et al.* 2019).

Of the different types of light source used in photolytics reactors for photodegradation processes, light emitting diodes (LEDs) can act as an alternative to conventional light sources owing to the fact that they require less energy and have a long service life (Xiong *et al.* 2020; Zhong *et al.* 2020). They also have the following advantages: low heating time; they do not require a special circuit; they are more

compact and they have no mercury disposal problems (Seidmohammadi *et al.* 2018; Wang *et al.* 2019a, 2019b).

When evaluating AOP processes, the study of toxicity is also of paramount importance, because if the organic contaminate is partially mineralized, it can be oxidized to other more biologically active or more toxic species, thus implying even more environmental hazards (Kanakaraju *et al.* 2018).

In addition to toxicity studies, it is also necessary to evaluate the influence of parameters on the efficiency of the degradation process. According to Villota *et al.* (2018), some parameters that can influence the photo-Fenton process are the pH, the light intensity and the concentrations of hydrogen peroxide (H_2O_2), and iron ions (Fe^{2+}). In this context, the proposition of empirical mathematical models is interesting, since they make it possible to predict the percentage of degradation of the contaminant as a function of the variables involved in the process. However, the analysis and estimation of these variables are necessary to enable their use in ideal conditions (Cabrera Reina *et al.* 2015).

The objective of this work was to compare the efficiency of LED and UV-C photo-reactors for paracetamol degradation when using the photo-peroxidation and photo-Fenton processes. Therefore, the behavior of the kinetic evolution of degradation and the toxicity of the compounds were evaluated before and after treatment with AOP processes through the use of seeds and bacteria. In addition, empirical mathematical models were proposed to predict paracetamol degradation, based on the results of the 2^4 full factorial designs and taking into account the behavior of the variables involved in the processes.

MATERIALS AND METHODS

Drug and reagents

The active ingredient of the drug paracetamol (lot: 18J24-B002-040227) was provided by the local handling pharmacy and used in the preparation of the stock solution ($100 \text{ mg}\cdot\text{L}^{-1}$). Dilutions were made from this solution in order to obtain the working solution ($10 \text{ mg}\cdot\text{L}^{-1}$) and to construct the analytical curves.

All the reagents used in this study were of the highest purity and were used without any purification. The source of iron was ferrous sulfate heptahydrate ($\text{FeSO}_4\cdot 7\text{H}_2\text{O}$, 99.98% purity, Vetec), while the oxidizing agent was hydrogen peroxide (H_2O_2 , 30% v/v, Modern Chemistry, standardized). The pH of the solutions was adjusted using

H_2SO_4 $1.0 \text{ mol}\cdot\text{L}^{-1}$ (97% purity, Merck) with the aid of a pH meter (Quimis, Q400AS).

Analytical methodology

Spectrophotometry ultraviolet/visible (UV/Vis)

The drug working solution ($10.0 \text{ mg}\cdot\text{L}^{-1}$) was subjected to spectral scanning between 190 and 1,100 nm, at different pH values, in order to assess whether there was a peak displacement (Figure 1).

Figure 1 shows two wavelengths (λ) at 197 and 243 nm, which are attributed to the $\pi\text{-}\pi^*$ transitions of the aromatic ring and to the $\pi\text{-}\pi^*$ transitions of the carbonyl group, respectively. It is also observed that there was no displacement of the λ studied as a function of the initial pH of the solution.

In this way, it was possible to construct the analytical curves, which presented a limit of detection (LD) of $0.05 \text{ mg}\cdot\text{L}^{-1}$, limit of quantification (LQ) of $0.20 \text{ mg}\cdot\text{L}^{-1}$, with coefficient of variation (CV) of 2.30% and correlation coefficient of 0.99.

High-performance liquid chromatography (HPLC)

In order to evaluate the efficiency of the process, paracetamol degradation was also monitored after 60, 120 and 180 min of treatments using HPLC (Shimadzu) equipped with a reverse mode Ultra C18 column ($5 \mu\text{m}$, $250 \text{ mm} \times 4.6 \text{ mm}$) and a UV detector (SPD-20A), set at 243 nm. The mobile phase used was a mixture of acetonitrile/water acidified with 0.1% acetic acid (50/50 v/v). The furnace

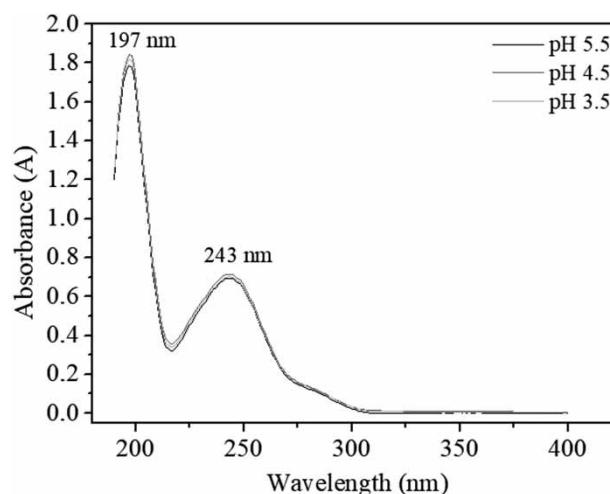


Figure 1 | Spectral scanning of paracetamol solution at different pH.

temperature of the equipment was maintained at 40 ± 1 °C with a flow of $0.9 \text{ mL}\cdot\text{min}^{-1}$ and a pressure of $104 \text{ kgf}\cdot\text{cm}^{-2}$.

Photo-reactors

In this work two benchtop photolytic reactors were used. To build the LED photo-reactor, a wooden box with a lid was used, because, according to Crittenden *et al.* (2012), photolytic reactors must be designed in order to ensure that all light sources used in the processes remain inside the reactor, in order to be absorbed by the species under study.

The photo-reactor was equipped with three LED lamps, arranged in parallel at the bottom of the cover, with a full power of 30 W and a photon emission of $3.9 \times 10^6 \mu\text{W}\cdot\text{cm}^{-2}$ in the visible range and $28 \mu\text{W}\cdot\text{cm}^{-2}$ in the UV-A/UV-B range. After construction of the reactor, it was coated with aluminum foil, aiming at greater radiation efficiency, as observed by Khan & Tahir (2019). The schematic drawing of the LED photo-reactor can be seen in Figure 2.

The UV-C photo-reactor, described and used by Zaidan *et al.* (2017a), was equipped with three UV-C lamps, arranged in parallel, with a total power of 90 W and a photon emission of $17.8 \text{ W}\cdot\text{m}^{-2}$.

Preliminary study

In order to select the most efficient system (AOP/radiation) as regards paracetamol degradation, the photo-peroxidation and photo-Fenton processes were initially tested using the two photo-reactors described above.

The experiments were conducted at 25 ± 1 °C at 120 min using: an iron concentration ($[\text{Fe}] = 1.0 \text{ mg}\cdot\text{L}^{-1}$); a hydrogen peroxide concentration ($[\text{H}_2\text{O}_2] = 27.0 \text{ mg}\cdot\text{L}^{-1}$); pH 5.5 (natural solution) for the photo-peroxidation process and pH 3.5 for the photo-Fenton process. The experiments were carried out by employing 100 mL capacity beakers to which 50 mL of the drug solution ($10 \text{ mg}\cdot\text{L}^{-1}$) were added. These conditions were selected on the basis of studies by Monteiro *et al.* (2018) and Santos *et al.* (2020), who investigated the degradation of the nimesulide, ibuprofen, ketoprofen, meloxicam and tenoxicam drugs using the photo-Fenton process.

Kinetic evaluation of paracetamol degradation

The kinetic study was evaluated by means of paracetamol degradation and the experiments were carried out in: 10;

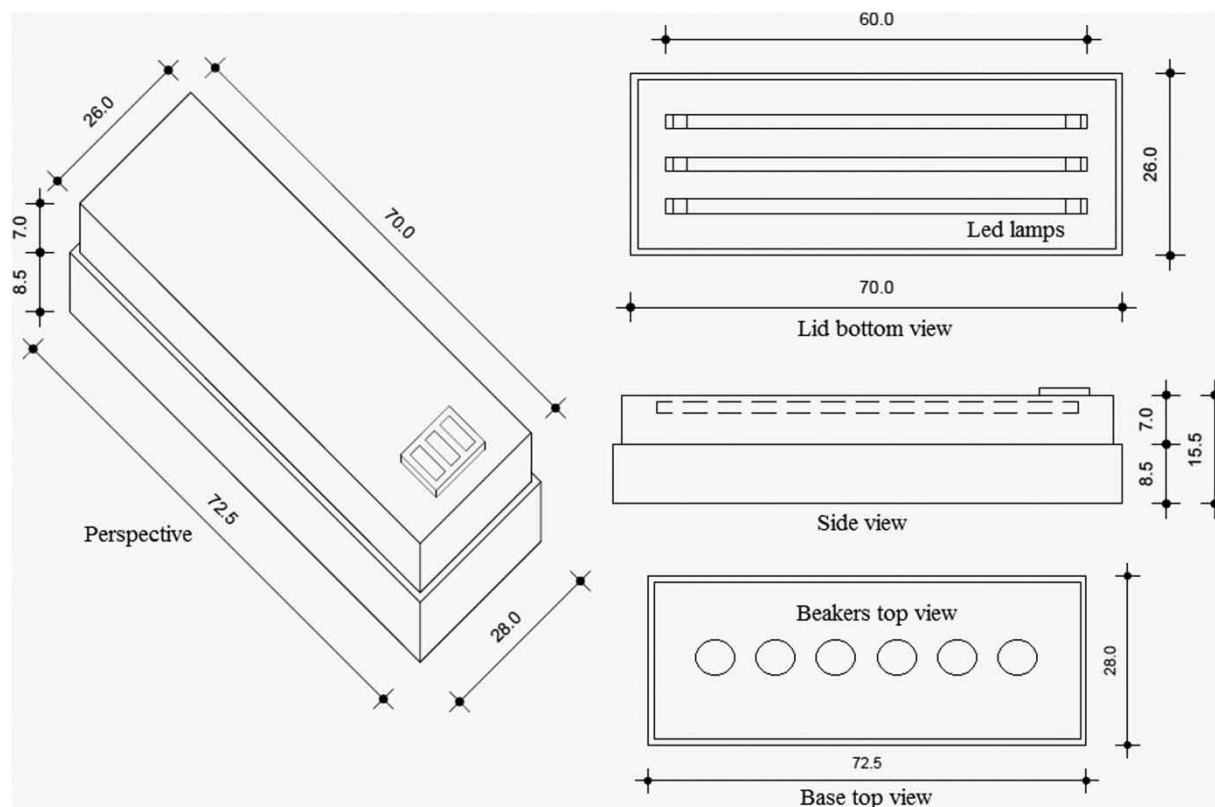


Figure 2 | Schematic drawing of the LED photo-reactor (measurements in cm).

20; 30; 45; 60; 90; 120; 150 and 180 min. The assays were performed using the most efficient systems, at a temperature of 25 ± 1 °C, using 100 mL capacity beakers, to which 50 mL of the drug solution were added. In addition, the kinetic evolution was monitored by means of spectral scanning in the range between 190 and 400 nm from 60 min onward.

The Chan and Chu model (Chan & Chu 2003) is currently being applied to describe the behavior of the kinetic evolution of drug degradation through the use of advanced oxidative processes. Santos *et al.* (2020) used this model to evaluate the degradation kinetics of the drugs ketoprofen, meloxicam and tenoxicam via the photo-Fenton process. Santana *et al.* (2019) made use of this model in the study of the photocatalytic oxidation of clozapine. This kinetic model, presented in Equation (1), was then adjusted to the experimental data.

$$C = C_0 \left(1 - \frac{t}{\rho + \sigma t} \right) \quad (1)$$

in which: C is the concentration of the drug ($\text{mg}\cdot\text{L}^{-1}$) after a time t (min) and C_0 is the initial concentration of the drug ($\text{mg}\cdot\text{L}^{-1}$). The parameters ρ and σ represent the reactional kinetics (min) and the oxidation capacity of the system (dimensionless), respectively.

The derivation of Equation (1) with time allows us to obtain Equation (2):

$$\frac{dC/C_0}{dt} = \frac{-\rho}{(\rho + \sigma t)^2} \quad (2)$$

According to Chan & Chu (2003), the higher the ratio $1/\rho$ ($t=0$), the faster the initial degradation of the compound studied. When t tends toward infinity, the value of the constant $1/\sigma$ equals the maximum oxidation capacity of the process at the end of the reaction.

Kinetic modeling was performed using a non-linear regression method (minimum squares method), employing Origin software (Version 8.0). The results of the adjustment were evaluated through the use of the linear regression coefficients (R^2).

The concentration of residual hydrogen peroxide was determined using a semi-quantitative colorimetric method with MQuant Test Strips (Merck). The test was performed at the end of the reaction kinetics experiment (180 min).

Toxicity study

Seed toxicity

The toxicity tests were performed under the same conditions as those employed in the kinetic study after 180 min for the most efficient systems. The toxicity evaluation consisted of the exposure of lettuce seeds (*Lactuca sativa*) to paracetamol solution before and after treatments. The assays were performed in triplicate, according to the methodology proposed by Zaidan *et al.* (2017b).

After the period of the test, the number of seeds that had germinated in the positive and negative controls was evaluated, and compared to the quantity that had germinated in the samples on each plate. Root growth was later observed, the size of whose radicles was measured with the aid of a pachymeter. The relative growth (RGI) and germination (GI) indices, provided in Equations (3) and (4), respectively, were, therefore, calculated and the results were evaluated according to Young *et al.* (2012).

$$RGI = \frac{RLS}{RLC} \quad (3)$$

$$GI = RGI \frac{(GSS)}{(GSC)} \quad (4)$$

in which: RLS is the total root length of the sample, RLC is the total root length in the negative control, GSS is the number of germinated seeds in the sample, and GSC is the number of germinated seeds in the negative control.

In order to better evaluate the toxicity of the compound under study, another study was carried out with two bacteria under the same conditions as those employed in the seed test.

Bacterial toxicity

With regard to the bacterial toxicity, the *Escherichia coli* UFPEDA 224 and *Salmonella enteritidis* UFPEDA 414 bacteria were cultured in a Mueller Hinton agar medium (MHA) at 36 °C. The colonies were subsequently resuspended in sterile saline solution (NaCl $0.15 \text{ mol}\cdot\text{L}^{-1}$) and adjusted turbidimetrically at a wavelength of 600 nm (OD_{600}) to obtain a suspension equivalent to 10^5 colony forming units (CFU) per mL. The samples were filtered on $13 \text{ mm} \times 0.22 \mu\text{m}$ sterile PVDF syringe filters. The assays were performed with the drug solution before and after treatments, as described by Nascimento *et al.* (2018).

It is important to note that *Escherichia coli* has been used as a bioreporter for the development of new ecotoxicological tests. Robbens *et al.* (2010) point out that the use of this bacterium as a bioindicator brings a sensitive and specific response, quickly. The authors further state that the use of 96-well microtiter is ideal for assessing the toxicity of a given sample.

Complementary analyses

The evaluation of the systems used in paracetamol degradation was complemented by analyzing the solutions before and after treatments for each of the parameters: conductivity, dissolved oxygen (DO), chemical oxygen demand (COD) and biochemical oxygen demand (BOD). The DO, COD and BOD analyses were carried out according to the 4500G, 5220D and 5210B methodologies described in *Standard Methods for the Examination of Water and Wastewater*, respectively (APHA 2012).

Empirical mathematical model to predict paracetamol degradation

2⁴ full factorial designs with a central point were performed with the objective of proposing an empirical model with which to predict the percentage of paracetamol degradation as a function of the variables involved in the processes (photo-Fenton with UV-C and LED radiations). With regard to the photo-Fenton/UV-C system, the variables whose influence on the process was evaluated were [H₂O₂] (27.0; 40.0 and 53.0 mg·L⁻¹), [Fe] (0.5, 0.75 and 1.0 mg·L⁻¹), pH (3.5, 4.5 and 5.5) and time (30, 60 and 90 min). Based on the results of this planning, the variables studied for the photo-Fenton/LED system were [H₂O₂] (27.0; 40.0 and 53.0 mg·L⁻¹), [Fe] (0.5, 0.75 and 1.0 mg·L⁻¹), time (30, 60 and 90 min) and power (10, 20 and 30 W). The response used to evaluate the efficiency of the process employed was the percentage of degradation of the drug. The tests were performed in random order and the central point in triplicate, totaling 19 experiments. The experiments were conducted at 25 ± 1 °C in a period of 60 min, using 50 mL of the solution in the concentration of 10 mg·L⁻¹ of the drug.

Paracetamol degradation by factorial design was assessed using a two-way analysis of variance (ANOVA), using the Statistica software 10.0, and considering the linear (L) and quadratic (Q) effects to a confidence level of 95%. The profiles of each of the variables studied were obtained for each λ using the Desirability function and an

empirical mathematical model was then proposed, using the behavior of these variables as a basis.

RESULTS AND DISCUSSION

Preliminary study

The results of the paracetamol degradation obtained using the photo-peroxidation and photo-Fenton processes with LED and UV-C radiations are included in the supplementary material (Table S1).

Kinetic evaluation of paracetamol degradation

The kinetic evaluation was carried out under the following conditions: [H₂O₂]: 27.0 mg·L⁻¹; [Fe]: 1.0 mg·L⁻¹; pH: 3.5, for the two systems (photo-Fenton/LED and photo-Fenton/UV-C). Figure 3 shows the fits of experimental data to the Chan and Chu kinetic model, relative to the decay of the C/C₀ ratio during the oxidation process of the groups that are absorbed in the λ of 197 and 243 nm of the paracetamol molecule.

Figure 3(a) and 3(c) make it possible to verify that, after 90 and 120 min of treatment using the photo-Fenton/UV-C and photo-Fenton/LED systems, respectively, there was no significant difference in the degradation of paracetamol under the conditions studied. The degradations obtained for the photo-Fenton/UV-C system were 82 and 94% for groups absorbed in the λ of 197 and 243 nm, respectively. In the case of the photo-Fenton/LED system, the degradation values were 81 and 91%, respectively. It is important to stress that the total power of the LED photo-reactor is three times lower than the total power of the UV-C photo-reactor, thus demonstrating the potential of using LED radiation.

Villota *et al.* (2016) investigated the application of the photo-Fenton process with a UV lamp (150 W) for the degradation of paracetamol (100 mg·L⁻¹) and obtained 100% degradation after 40 min. However, [H₂O₂] of 220 mg·L⁻¹ and [Fe] of 20 mg·L⁻¹ were used, which are much greater quantities than those used in this work. Moreover, the power employed was five times greater than that used in this work (LED radiation).

It is important to stress those high concentrations of [H₂O₂] and high power lamps result in increased operating costs for the treatment. Excess iron can make the solution cloudy, thus inhibiting the absorption of radiation by the contaminant.

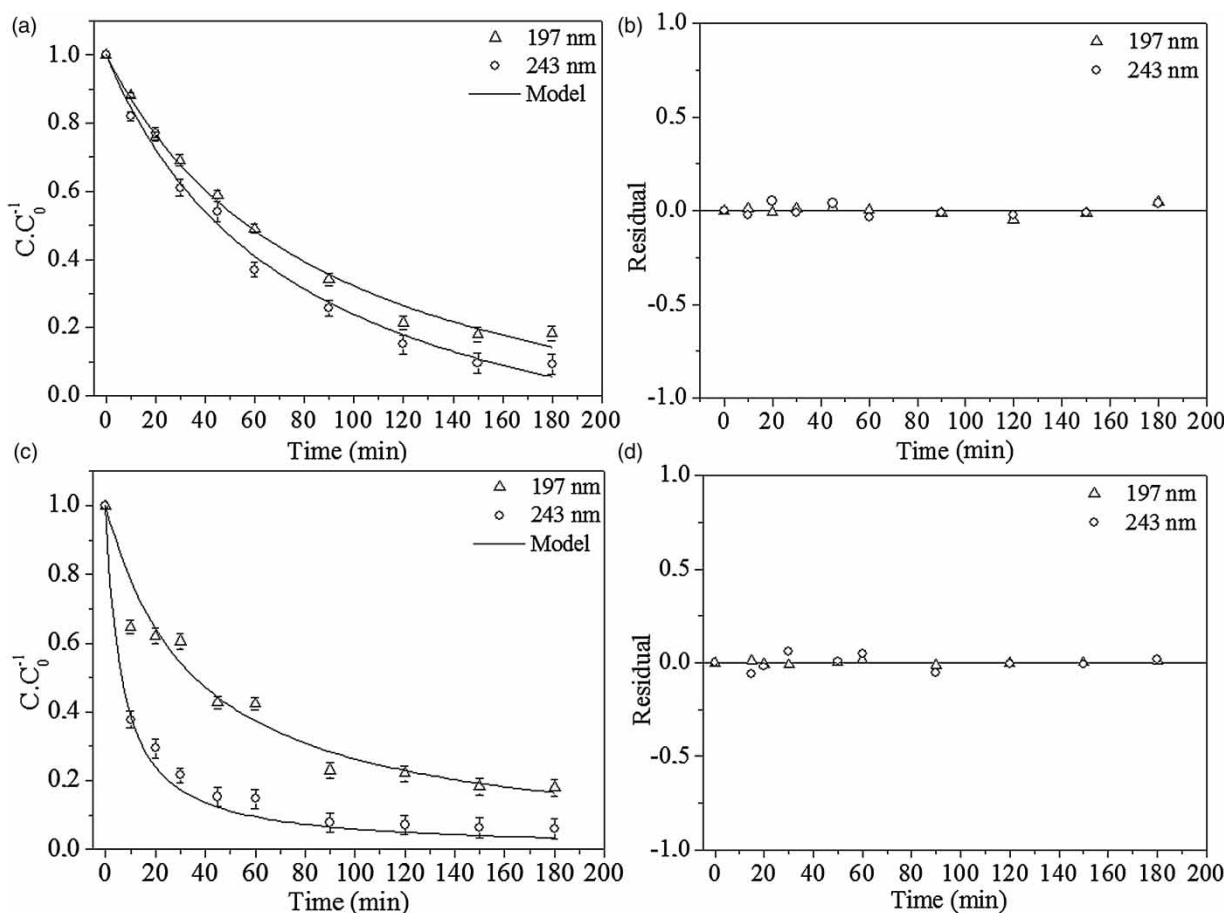


Figure 3 | Kinetic evaluation of paracetamol degradation by photo-Fenton/LED and photo-Fenton/UV-C systems: (a) and (c) adjusting the kinetic model; (b) and (d) residual graphs, respectively.

Upon analyzing [Figure 3\(b\)](#) and [3\(d\)](#), it will be noted that the residual distribution was shown to be random with low values (± 0.001), indicating a good adjustment of the experimental values to those calculated by the Chan & Chu model (2003), which can be confirmed by the values of the coefficients of linear regression presented in [Table 1](#). This good fit indicates that the degradation of paracetamol has pseudo-first order behavior. The other kinetic parameters of the oxidation reaction obtained from Equations (1) and (2) can be observed in [Table 1](#).

Table 1 | Kinetic parameters

System λ (nm)	Photo-Fenton/LED			Photo-Fenton/UV-C		
	$1/\rho^a$	$1/\sigma^b$	r	$1/\rho^a$	$1/\sigma^b$	r
197	0.013	1.10	0.99	0.017	1.00	0.98
243	0.018	1.12	0.99	0.028	1.02	0.99

$1/\rho^a$: the initial rates; $1/\sigma^b$: the maximum oxidation capacity.

[Table 1](#) shows that the initial removal rate ($1/\rho$) was higher for the wavelength of 243 nm in the case of both systems, and obtained a faster decrease ratio of this compound, which is confirmed by [Figure 3\(a\)](#) and [3\(c\)](#). The maximum oxidation capacity of the system ($1/\sigma$) was similar for all the λ studied. The values of $1/\rho$ and $1/\sigma$ were in the same order of magnitude for both of the systems evaluated.

Spectral scanning in the range of 190–400 nm of the kinetic study samples from 60 min onward was then performed, which is presented in [Figure 4](#).

In [Figure 4\(a\)](#) and [4\(b\)](#), it is possible to observe a gradual reduction in the peak amplitude with regard to the λ of 197 nm for both the systems studied; however, the photo-Fenton/UV-C system was able to reduce the amplitude of that peak more rapidly. The peak representing the λ of 243 nm disappeared after 60 min of treatment when using the photo-Fenton/UV-C system and after 90 min in the case of the photo-Fenton/LED system. The formation of

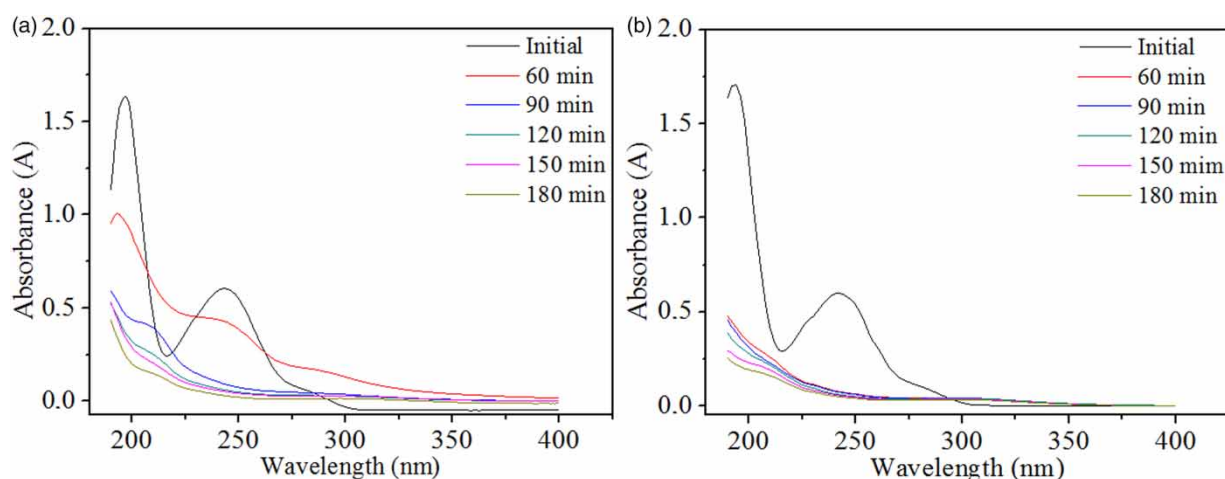


Figure 4 | Spectral monitoring of kinetics degradation by systems: (a) photo-Fenton/LED and (b) photo-Fenton/UV-C.

new peaks was not identified by the spectrophotometry UV-Vis technique for the wavelength range studied. At the end of each treatment, the concentration of residual hydrogen peroxide was, therefore, analyzed and the result found was in the range of $0.5\text{--}2\text{ mg}\cdot\text{L}^{-1}$, showing that almost all of the hydrogen peroxide was consumed during the reaction.

The chromatograms obtained for the paracetamol solution ($10.0\text{ mg}\cdot\text{L}^{-1}$) before and after treatments using the photo-Fenton/UV-C and photo-Fenton/LED systems are shown in Figure 5.

The retention time for the paracetamol (Figure 5(a)) was similar to that found in literature (Jallouli *et al.* 2017), which allows confirmation of the identification of the compound.

With regard to the photo-Fenton/LED system, Figure 5(b) shows a significant reduction in peak intensity after 60 min of treatment, which corroborates the result obtained by spectral monitoring using UV-Vis spectrophotometry, shown in Figure 4. The formation of a peak at the retention time of approximately 11.3 min can be further verified in Figure 5(b). However, after 120 min of treatment (Figure 5(c) and 5(d)), this peak was not observed. Peak area reductions of 79.3%, 88.8% and 90.6% were obtained after 60, 120 and 180 min, respectively.

An analysis of Figure 5(e)–5(g), for the photo-Fenton/UV-C system, shows that the peaks disappeared after 60 min of treatment. As described by Slamani *et al.* (2018), the paracetamol ($\text{C}_8\text{H}_9\text{NO}_2$) degradation process via the photo-Fenton process occurs in three stages until it reaches complete mineralization, as can be seen in Equation (5).



in which:

$A = \text{C}_6\text{H}_6\text{O}_2$ (hydroquinone, resorcinol, catechol-position isomers)

$B = \text{C}_6\text{H}_4\text{N}_2\text{O}_5$ (2,4 dinitrophenol)

$C = \text{C}_6\text{H}_4\text{O}_2$ (para-benzoquinone)

$$D = \begin{cases} \text{C}_2\text{H}_2\text{O}_4 \text{ (oxalic acid)} \\ \text{C}_4\text{H}_4\text{O}_4 \text{ (fumaric acid)} \\ \text{C}_2\text{H}_4\text{O}_2 \text{ (acetic acid)} \\ \text{CH}_2\text{O}_2 \text{ (metanoic acid)} \\ \text{C}_2\text{H}_2\text{O}_5 \text{ (ketomalonic)} \end{cases}$$

Toxicity study

Seed toxicity

The toxicity of the solutions before and after submission to the two systems was evaluated as regards *Lactuca sativa* seeds. This was done by counting the number of seeds that germinated and their root growth, and by calculating the relative growth (RGI) and germination (GI) indices. The obtained results are set out in Table 2.

An analysis of Table 2 shows that the germination and the root growth of the seeds for the solution after the treatment were higher than for the solution before the treatment. Similar behavior was observed for GI and RGI. The solutions after the treatments had an RGI greater than 0.80, which, according to Young *et al.* (2012), does not show growth inhibition. It was also found that the best results were obtained when employing the photo-Fenton/LED system.

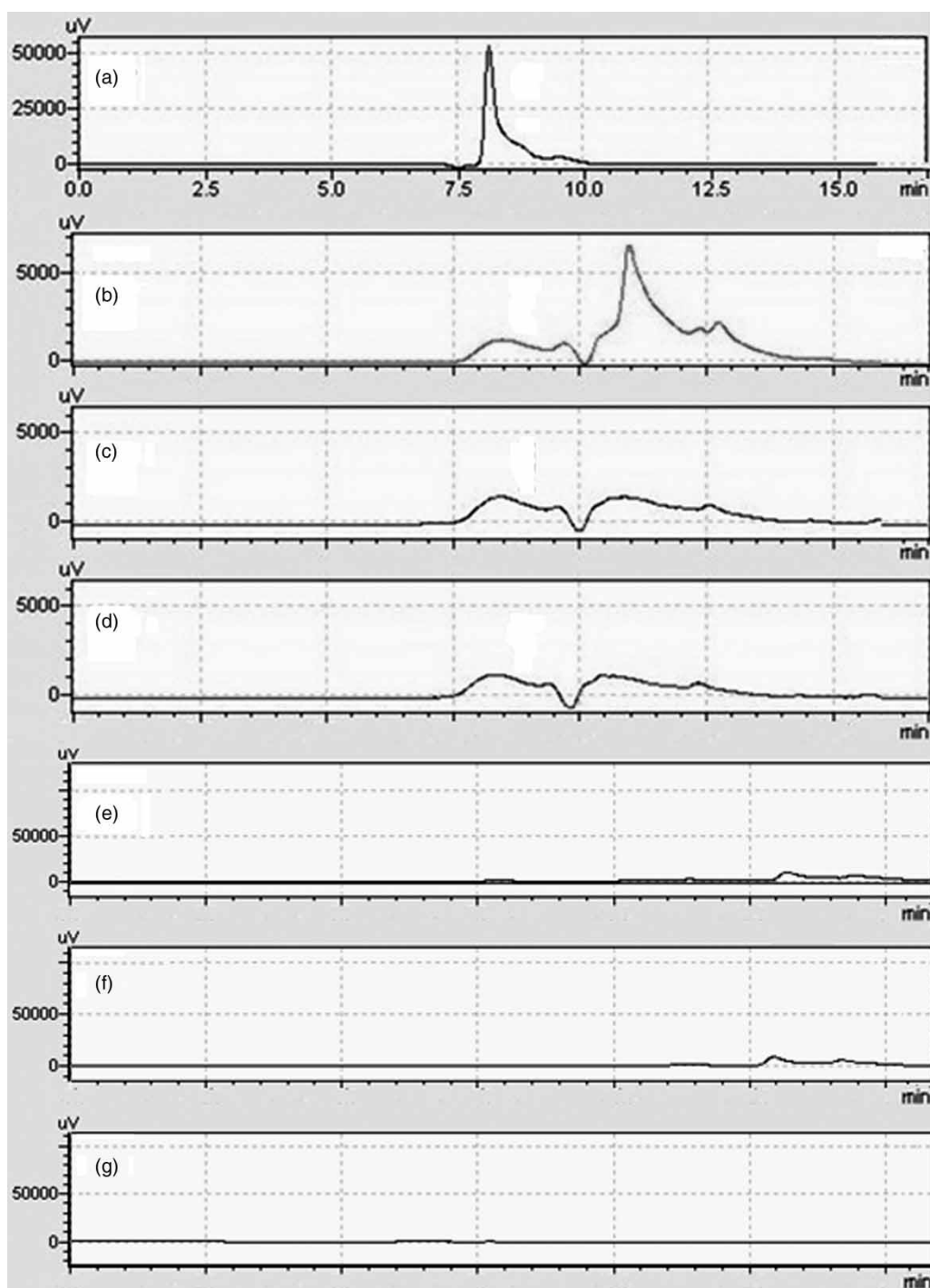


Figure 5 | Chromatograms of the paracetamol solution: (a) before treatment; after photo-Fenton/LED: (b) 60 min, (c) 120 min and (d) after 180 min; after photo-Fenton/UV-C: (e) 60 min, (f) 120 min and (g) 180 min.

When assessing the toxicity of an aqueous solution containing ketoprofen, tenoxicam and meloxicam submitted to the photo-Fenton process, Santos *et al.* (2020) observed that solutions after treatment negatively influenced the growth of *Veneranda* lettuce seeds.

Bacterial toxicity

The results of the mean and standard deviation (SD) of the bacterial activity of the samples for OD_{600} after 24 hours of incubation are shown in Table 3.

Table 2 | Results of the toxicity test using *Lactuca sativa* seeds for the two systems

Sample	Average of the seeds that germinated	Root growth		
		Mean \pm SD ^c (cm)	RGI	GI (%)
Negative control	9.67 \pm 0.58	5.95 \pm 0.92	1.00	100.00
SBT ^a	4.67 \pm 1.51	2.40 \pm 1.19	0.40	19.47
SAT ^b (LED)	9.43 \pm 0.58	5.27 \pm 0.70	0.90	90.29
SAT ^b (UV-C)	8.33 \pm 0.58	3.63 \pm 1.20	0.81	72.64

SBT^a, solution before treatment; SAT^b, solution after treatment; SD^c, standard deviation.

Table 3 | Results of bacterial toxicity using *Escherichia coli* and *Salmonella enteritidis* bacteria for the two systems

Samples	Mean \pm SD ^c (OD ₆₀₀)	
	<i>Escherichia coli</i>	<i>Salmonella enteritidis</i>
Negative control	0.14 \pm 0.05	0.29 \pm 0.01
SBT ^a	0.16 \pm 0.01	0.175 \pm 0.002
SAT ^b (LED)	0.18 \pm 0.05	0.156 \pm 0.009
SAT ^b (UV-C)	0.19 \pm 0.04	0.105 \pm 0.006

SBT^a, solution before treatment; SAT^b, solution after treatment; SD^c, standard deviation.

An analysis of [Table 3](#) shows that, according to the OD₆₀₀ values, the bacterial growth of *Escherichia coli* strains had values higher than those of the negative control for solutions before and after treatment. This result indicates that there was no inhibition of growth of this bacterium in the case of either of the two systems studied. With regard to the bacterial strains of *Salmonella enteritidis*, growth inhibition was observed for the samples before and after treatment, because they had lower bacterial growth values than the negative control for both systems studied. This bacterium was, therefore, sensitive to the samples evaluated.

These same bacteria (*Escherichia coli* and *Salmonella enteritidis*) were used by [Santana *et al.* \(2019\)](#) to evaluate the toxicity of clozapine drug-containing solutions before and after treatment with photocatalytic oxidation using supported TiO₂. The results of the toxicological tests showed growth inhibition for all the samples, indicating that the products generated by the reaction were more toxic than the original compound.

Complementary analyses

The results of the physicochemical analysis of the solutions before and after the treatments using both systems are presented in [Table 4](#).

Table 4 | Results of the physicochemical analysis

Parameters	Before treatment	After treatment (LED)	After treatment (UV-C)
Conductivity ($\mu\text{S}\cdot\text{cm}^{-1}$)	11.70	653	598
DO ($\text{mg O}_2\cdot\text{L}^{-1}$)	6.0	5.98	5.86
COD ($\text{mg O}_2\cdot\text{L}^{-1}$)	23.8	4.95	5.23
BOD ($\text{mg O}_2\cdot\text{L}^{-1}$)	< 2.0	< 2.0	< 2.0

According to [Table 4](#), the conductivity increased significantly after the treatments, which may be related to the degradation of the drug molecule, which leads to an increase in organic and inorganic ions in the solution. Dissolved oxygen (DO) remained constant after the treatments, since the processes had no aeration system. The BOD of all the samples was below the method quantification limit. It was also observed that there was a reduction in COD values for both treatments, demonstrating a reduction in the amount of non-biodegradable organic matter present in the solution.

Empirical mathematical model to predict paracetamol degradation

The effect estimates obtained after employing a two-way ANOVA analysis for paracetamol degradation using the photo-Fenton/UV-C and photo-Fenton/LED systems with a confidence interval of 95% are shown in supplementary material ([Table S2](#)).

The results indicate a good fit of the experimental data to the model according to the high values of R² and the low values of MS pure error for both λ (197 and 243 nm) when using the two systems. The effects [Fe] (Q), pH (Q) and Time (Q) were a linear combination of other effects and were not estimated for either λ at a confidence interval of 95%.

Considering that the best paracetamol degradation result for the photo-Fenton/UV-C system was obtained using the lowest pH (3.5) and according to [Feng *et al.* \(2013\)](#), better results are obtained for the Fenton processes at this pH, so it was decided to keep the pH constant at 3.5 and to evaluate the lamp power variable for the photo-Fenton/LED system.

In the case of both systems, the main effects [H₂O₂] (Q) (negative) and Time (L) (positive) made the greatest contributions to paracetamol degradation, at both 197 nm and at 243 nm. The negative effect of [H₂O₂] (Q) may possibly be attributed to the fact that, according to [Araújo *et al.*](#)

(2006), when present in excess in the reaction, this reagent can act as a quench of the hydroxyl radicals, thus disfavoring the reactions of degradation of the compound and the organic matter. However, the positive effect of Time (L) is related to the fact that the longer the exposure time to the higher radiation, the higher the percentage of degradation obtained.

According to the p -value ≤ 0.05 for the photo-Fenton/UV-C system, the effects [Fe] (L) and [H₂O₂] (L) by pH (L) for 197 nm; [H₂O₂] (L) by [Fe] (L) and [H₂O₂] (L) by pH (L) for 243 nm were not significant at a confidence interval of 95%, and were, therefore, discarded from the model. With regard to the photo-Fenton/LED system, all the effects were significant within a confidence interval of 95% for both λ . This sequence allowed us to determine the desirability of the effects and percentage of the models for each wavelength, as shown in Figure 6.

In the case of the photo-Fenton/UV-C system, the results indicated a maximum percentage of desirability of the model from 69.70% to 197 nm and 90.76% to 243 nm. Upon

considering all the effects, the average desirability of 82% was obtained for the λ of 197 nm under the conditions: [H₂O₂] = 40 mg·L⁻¹; [Fe] = 0.75 mg·L⁻¹; pH = 4.5; Time = 60 min. In the case of 243 nm, the average desirability was 73% under the same conditions. The results obtained using the photo-Fenton/LED system showed a maximum percentage of desirability of the model of 77.09% and 90.52% for 197 and 243 nm, respectively. With regard to the λ of 197 nm, the average desirability obtained was 78% under the conditions: [H₂O₂] = 40 mg·L⁻¹; [Fe] = 0.75 mg·L⁻¹; Time = 60 min and Power = 20 W. In the case of 243 nm, this average desirability was 73% under the same conditions.

The contribution of the effect of [H₂O₂] was parabolic for both systems (with a maximum of around 40 mg·L⁻¹). The contribution of [Fe] to the degradation did not change for the photo-Fenton/UV-C system, while it increased for the photo-Fenton/LED system. The contribution of the effect of Time was found to increase for both systems. Finally, the contributions of the effects of pH

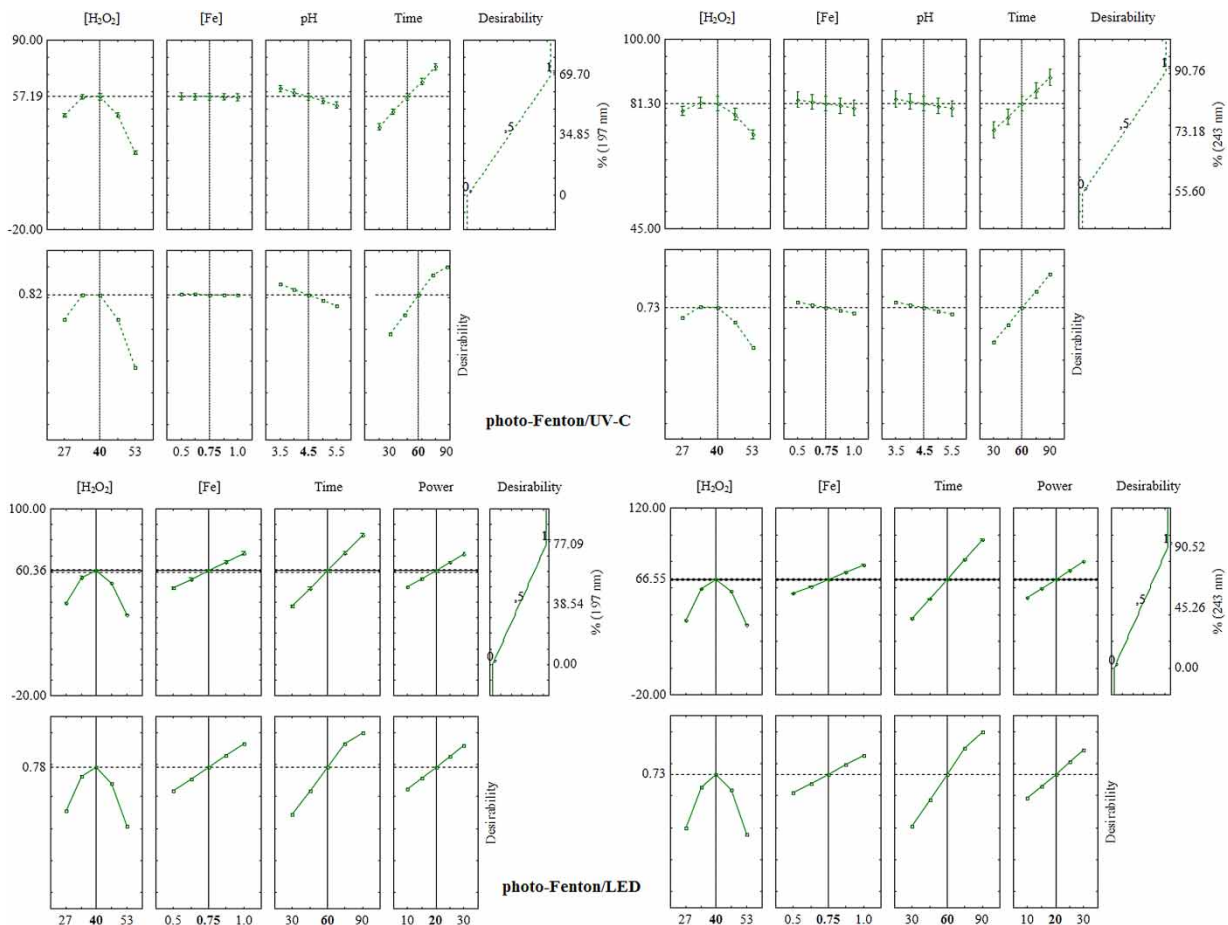


Figure 6 | Desirability and percentage of the model for 197 and 243 nm using photo-Fenton/UV-C and photo-Fenton/LED systems.

(photo-Fenton/UV-C system) and Power (photo-Fenton/LED system) decreased and increased, respectively.

In order to simplify the prediction of paracetamol degradation in terms of the effects evaluated, and based on the behavior of the observed desirability, the empirical models presented in Equations (6) and (7) were proposed for the photo-Fenton/UV-C and photo-Fenton/LED systems, respectively. In these equations, the parabolic behavior of the $[H_2O_2]$ effect generated a quadratic term, and the increasing (Time, Power and $[Fe]$) and constant ($[Fe]$) behaviors provided positive terms. The contribution of the pH effect (decreasing) generated an inversely proportional term.

$$\text{Degradation}(\%) = \frac{A * [H_2O_2]^2 * [Fe] * \text{Time}}{pH} + B \quad (6)$$

$$\text{Degradation}(\%) = A * [H_2O_2]^2 * [Fe] * \text{Time} * \text{Power} + B \quad (7)$$

in which: t (min) is the time and A and B are the constants of the model.

The adjustment of the experimental data for the λ of 197 and 243 nm to the models (least squares as a loss function) at a confidence interval of 95%, resulted in unsatisfactory predictions. Another empirical model was subsequently proposed, according to Equations (8) and (9), for the photo-Fenton/UV-C and photo-Fenton/LED systems, respectively.

$$\text{Degradation}(\%) = A * [H_2O_2]^{k_1} * [Fe]^{k_2} * pH^{k_3} * \text{Time}^{k_4} + B \quad (8)$$

$$\text{Degradation}(\%) = A * [H_2O_2]^{k_1} * [Fe]^{k_2} * \text{Time}^{k_3} * \text{Power}^{k_4} + B \quad (9)$$

in which: A , B and k_i ($i = 1, 2, 3, 4$) are the constants of the models.

The values of the fit constants of the models (Equations (8) and (9)), when considering least squares as a loss function at a confidence interval of 95%, are shown in Table 5.

The results in Table 5 indicate a good fit of the experimental data to the proposed models. The orders of magnitude observed for parameters A and B were significantly different in the case of the two λ . However, despite being simpler and obtaining satisfactory results, it should be emphasized that the use of the model for the photo-Fenton/UV-C system was restricted to the levels of $27.0 \text{ mg} \cdot \text{L}^{-1} \leq [H_2O_2] \leq 53.0 \text{ mg} \cdot \text{L}^{-1}$; $0.5 \text{ mg} \cdot \text{L}^{-1} \leq [Fe] \leq 1.0 \text{ mg} \cdot \text{L}^{-1}$; $3 \leq \text{pH} \leq 6$ and $30 \text{ min} \leq \text{Time} \leq 90 \text{ min}$. In the case of the photo-Fenton/LED system, it was restricted to the levels of $27.0 \text{ mg} \cdot \text{L}^{-1} \leq [H_2O_2] \leq 53.0 \text{ mg} \cdot \text{L}^{-1}$; $0.5 \text{ mg} \cdot \text{L}^{-1} \leq [Fe] \leq 1.0 \text{ mg} \cdot \text{L}^{-1}$; $30 \text{ min} \leq \text{Time} \leq 90 \text{ min}$ and $10 \text{ W} \leq \text{Power} \leq 30 \text{ W}$.

CONCLUSION

The photo-Fenton process combined with LED and UV-C radiation was more efficient when compared to photo-peroxidation for paracetamol degradation, under the conditions studied. The data obtained from the kinetic study of the two systems were well represented by the Chan and Chu model, with percentages of degradations greater than 81 and 91% (λ of 197 and 243 nm, respectively). No toxicity of the samples was observed when using *Lactuca sativa* seeds or strains of the bacterium *Escherichia coli* in the case of either of the systems. The *Salmonella enteritidis* bacterium strains were sensitive to the samples

Table 5 | Fit of experimental data to proposed models

Photo-Fenton/LED							
λ (nm)	Values of the constants \pm standard error						
	A	B	k_1	k_2	k_3	k_4	R^2
197	67 \pm 17	-146 \pm 23	-0.047 \pm 0.008	0.17 \pm 0.02	0.23 \pm 0.03	0.11 \pm 0.01	0.93
243	18 \pm 5	-101 \pm 13	-0.017 \pm 0.009	0.23 \pm 0.02	0.40 \pm 0.04	0.19 \pm 0.01	0.91
Photo-Fenton/UV-C							
λ (nm)	Values of the constants \pm standard error						
	A	B	k_1	k_2	k_3	k_4	R^2
197	706 \pm 65	-662 \pm 65	-0.014 \pm 0.005	0.001 \pm 0.000	-0.028 \pm 0.004	0.046 \pm 0.006	0.92
243	53 \pm 27	5 \pm 3	-0.11 \pm 0.05	-0.06 \pm 0.02	-0.07 \pm 0.03	0.20 \pm 0.08	0.90

before and after treatments. The empirical mathematical models proposed in this study were able to predict paracetamol degradation. These models could, therefore, be used to predict percentages of degradation in other studies as a function of the variables studied, using the same levels assessed. Both systems can, therefore, be considered viable treatments for paracetamol degradation, under the conditions studied. It is important to stress that the total power of the LED photo-reactor is three times lower than that of the UV-C photo-reactor, thus demonstrating the potential of LED radiation.

ACKNOWLEDGEMENTS

The authors would like to thank the Laboratory of Protein Biochemistry at the Universidade Federal de Pernambuco, Coordenação de Aperfeiçoamento de Pessoal de Nível Superior (CAPES), Fundação de Amparo a Ciência e Tecnologia de Pernambuco (FACEPE), Fundação de Apoio ao Desenvolvimento da Universidade Federal de Pernambuco (FADE/UFPE) and Núcleo de Química Analítica Avançada de Pernambuco-NUQAAPE (FACEPE, processo APQ-0346-1.06/14).

DATA AVAILABILITY STATEMENT

All relevant data are included in the paper or its Supplementary Information.

REFERENCES

- APHA 2012 *Standard Methods for the Examination of Water and Wastewater*, 22nd edn. American Public Health Association, Washington, DC.
- Araújo, F. V. F., Yokoyama, L. & Teixeira, L. A. C. 2006 **Color removal in reactive dye solutions by UV/H₂O₂ oxidation.** *Quim. Nova* **29**, 11–14. <http://dx.doi.org/10.1590/S0100-40422006000100003>.
- Beek, T. A. D., Weber, F.-A., Bergmann, A., Hickmann, S., Ebert, I., Hein, A. & Kuster, A. 2016 **Pharmaceuticals in the environment – global occurrences and perspectives.** *Environ. Toxicol. Chem.* **35**, 823–835. <https://doi.org/10.1002/etc.3339>.
- Cabrera Reina, A., Santos-Juanes, L., García Sánchez, J. L., Casas López, J. L., Maldonado Rubio, M. I., Li Puma, G. & Sánchez Pérez, J. A. 2015 **Modelling the photo-Fenton oxidation of the pharmaceutical paracetamol in water including the effect of photon absorption (VRPA).** *Appl. Catal. B* **166–167**, 295–301. <https://doi.org/10.1016/j.apcatb.2014.11.023>.
- Chan, K. H. & Chu, W. 2003 **Modeling the reaction kinetics of Fenton's process on the removal of atrazine.** *Chemosphere* **51**, 305–311. [https://doi.org/10.1016/S0045-6535\(02\)00812-3](https://doi.org/10.1016/S0045-6535(02)00812-3).
- Comber, S., Gardner, M., Sörme, P., Leverett, D. & Ellor, B. 2018 **Active pharmaceutical ingredients entering the aquatic environment from wastewater treatment works: a cause for concern?** *Sci. Total Environ.* **613–614**, 538–547. <https://doi.org/10.1016/j.scitotenv.2017.09.101>.
- Crittenden, J. C., Trussel, R. R., Hand, D. W., Howe, K. J. & Tchobanoglous, G. 2012 *MWH's Water Treatment: Principles and Design*. John Wiley & Sons, New Jersey, USA.
- Feier, B., Florea, A., Cristea, C. & Sandulescu, R. 2018 **Electrochemical detection and removal of pharmaceuticals in wastewaters.** *Curr. Opin. Electrochem.* **11**, 1–11. <https://doi.org/10.1016/j.coelec.2018.06.012>.
- Feng, L., Hullebusch, E. D. V., Rodrigo, M. A., Esposito, G. & Oturan, M. A. 2013 **Removal of residual anti-inflammatory and analgesic pharmaceuticals from aqueous systems by electrochemical advanced oxidation processes: a review.** *Chem. Eng. J.* **228**, 944–964. <https://doi.org/10.1016/j.cej.2013.05.061>.
- Jallouli, N., Elghniji, K., Trabelsi, H. & Ksibi, M. 2017 **Photocatalytic degradation of paracetamol on TiO₂ nanoparticles and TiO₂/cellulosic fiber under UV and sunlight irradiation.** *Arab. J. Chem.* **10**, S3640–S3645. <https://doi.org/10.1016/j.arabjc.2014.03.014>.
- Kanakaraju, D., Glass, B. D. & Oelgemoller, M. 2018 **Advanced oxidation process-mediated removal of pharmaceuticals from water: a review.** *J. Environ. Manage.* **219**, 189–207. <https://doi.org/10.1016/j.jenvman.2018.04.103>.
- Katic, V., Santos, P. L., Gabriel, J. G., Salomão, A. A. & Bonacin, J. A. 2018 **Assembly of low-cost lab-made photoreactor for preparation of nanomaterials.** *Quim. Nova* **41**, 105–109. <https://doi.org/10.21577/0100-4042.20170123>.
- Khan, A. A. & Tahir, M. 2019 **Recent advancements in engineering approach towards design of photoreactors for selective photocatalytic CO₂ reduction to renewable fuels.** *J. CO₂ Util.* **29**, 205–239. <https://doi.org/10.1016/j.jcou.2018.12.008>.
- Kowalska, K., Maniakova, G., Carotenuto, M., Sacco, O., Vaiano, V., Lofrano, G. & Rizzo, L. 2020 **Removal of carbamazepine, diclofenac and trimethoprim by solar driven advanced oxidation processes in a compound triangular collector-based reactor: a comparison between homogeneous and heterogeneous processes.** *Chemosphere* **238**, 124665. <https://doi.org/10.1016/j.chemosphere.2019.124665>.
- Lee, Y., Gerrity, D., Lee, M., Gamage, S., Pisarenko, A., Trenholm, R. A., Cononica, S., Snyder, S. A. & Von Gunten, U. 2016 **Organic contaminant abatement in reclaimed water by UV/H₂O₂ and a combined process consisting of O₃/H₂O₂ followed by UV/H₂O₂: prediction of abatement efficiency, energy consumption and byproduct formation.** *Environ. Sci. Technol.* **50**, 3809–3819. <https://doi.org/10.1021/acs.est.5b04904>.
- Lessa, E. F., Nunes, M. L. & Fajardo, A. R. 2018 **Chitosan/waste coffee-grounds composite: an efficient and eco-friendly adsorbent for removal of pharmaceutical contaminants from water.** *Carbohydr. Polym.* **189**, 257–266. <https://doi.org/10.1016/j.carbpol.2018.02.018>.

- Lofrano, G., Pedrazzani, R., Libralato, G. & Carotenuto, M. 2017 **Advanced oxidation processes for antibiotics removal: a review.** *Curr. Org. Chem.* **21**, 1–14. <https://doi.org/10.2174/1385272821666170103162813>.
- Monteiro, R. T., Santana, R. M. R., Silva, A. M. R. B., Lucena, A. L. A., Zaidan, L. E. M. C., Silva, V. L. & Napoleão, D. C. 2018 **Degradation of the pharmaceuticals nimesulide and ibuprofen using photo-Fenton process: toxicity studies, kinetic modeling and use of artificial neural networks.** *Electron. J. Manage., Edu. Environ. Technol.* **22** (e3), 1–21. <https://doi.org/10.5902/22361170>.
- Nascimento, G. E., Napoleão, D. C., Silva, P. K. A., Santana, R. M. R., Bastos, A. M. R., Zaidan, L. E. M. C., Moura, M. C., Coelho, L. C. B. B. & Duarte, M. M. M. B. 2018 **Photo-assisted degradation, toxicological assessment, and modeling using artificial neural networks of reactive gray BF-2R dye.** *Water Air Soil Pollut.* **229**, 379. <https://doi.org/10.1007/s11270-018-4028-2>.
- Nguyen, V.-H. & Wu, J. C. S. 2018 **Recent developments in the design of photoreactors for solar energy conversion from water splitting and CO₂ reduction.** *Appl. Catal. A-Gen.* **550**, 122–141. <https://doi.org/10.1016/j.apcata.2017.11.002>.
- Prasse, C., Stalter, D., Schulte-Oehlmann, U., Oehlmann, J. & Ternes, T. A. 2015 **Spoil for choice: a critical review on the chemical and biological assessment of current wastewater treatment technologies.** *Water. Res.* **87**, 237–270. <https://doi.org/10.1016/j.watres.2015.09.023>.
- Robbens, J., Dardenne, F., Devriese, L., De Coen, W. & Blust, R. 2010 ***Escherichia coli* as a bioreporter in ecotoxicology.** *Appl. Microbiol. Biotechnol.* **88**, 1007–1025. <https://doi.org/10.1007/s00253-010-2826-6>.
- Russo, D., Tammamo, M., Salluzzo, A., Andreozzi, R. & Marotta, R. 2019 **Modeling and validation of a modular multi-lamp photo-reactor for cetylpyridinium chloride degradation by UV and UV/H₂O₂ processes.** *Chem. Eng. J.* **376**, 120380. <https://doi.org/10.1016/j.cej.2018.11.078>.
- Santana, R. M. R., Moura, T. C. L., Nascimento, G. E., Charamba, L. C. V., Duarte, M. M. M. B. & Napoleão, D. C. 2019 **Photocatalytic oxidation of clozapine using TiO₂ immobilized in polystyrene: effect of operation parameters and artificial neural network modeling.** *Rev. Eletrônica Gest., Educ. Tecnol. Ambient.* **23**, 1–11. <https://doi.org/10.5902/2236117038236>.
- Santos, M. M. M., Silva, T. D., Lucena, A. L. A., Napoleão, D. C. & Duarte, M. M. M. B. 2020 **Degradation of ketoprofen, tenoxicam, and meloxicam drugs by photo-assisted peroxidation and photo-Fenton processes: identification of intermediates and toxicity study.** *Water Air Soil Pollut.* **231** (35), 1–15. <https://doi.org/10.1007/s11270-020-4401-9>.
- Seidmohammadi, A., Amiri, R., Faradmal, J., Lili, M. & Asgari, G. 2018 **UVA-LED assisted persulfate/nZVI and hydrogen peroxide/nZvi for degrading 4-chlorophenol in aqueous solutions.** *Korean J. Chem. Eng.* **35** (3), 694–701. <https://doi.org/10.1007/s11814-017-0317-5>.
- Serpone, N., Artemev, Y. M., Ryabchuk, V. K., Emeline, A. V. & Horikoshi, S. 2017 **Light-driven advanced oxidation processes in the disposal of emerging pharmaceutical contaminants in aqueous media: a brief review.** *Curr. Opin. Green. Sustain. Chem.* **6**, 18–33. <https://doi.org/10.1016/j.cogsc.2017.05.003>.
- Slamani, S., Abdelmalek, F., Ghezzer, M. R. & Addou, A. 2018 **Initiation of Fenton process by plasma gliding arc discharge for the degradation of paracetamol in water.** *J. Photochem. Photobio. A.* **359**, 1–10. <https://doi.org/10.1016/j.jphotochem.2018.03.032>.
- Villota, N., Lomas, J. M. & Camarero, L. M. 2016 **Study of the paracetamol degradation pathway that generates color and turbidity in oxidized wastewaters by photo-Fenton technology.** *J. Photochem. Photobiol.* **329**, 113–119. <https://doi.org/10.1016/j.jphotochem.2016.06.024>.
- Villota, N., Lomas, J. M. & Camarero, L. M. 2018 **Kinetic modelling of water-color changes in a photo-Fenton system applied to oxidate paracetamol.** *J. Photochem. Photobiol.* **356**, 573–579. <https://doi.org/10.1016/j.jphotochem.2018.01.040>.
- Wang, Z., Srivastava, V., Ambat, I., Safaei, Z. & Sillanpää, M. 2019a **Degradation of Ibuprofen by UV-LED/catalytic advanced oxidation process.** *J. Water Process. Eng.* **31**, 100808. <https://doi.org/10.1016/j.jwpe.2019.100808>.
- Wang, Z., Thuy, G. N. S. T., Srivastava, V., Ambat, I. & Sillanpää, M. 2019b **Photocatalytic degradation of an artificial sweetener (Acesulfame-K) from synthetic wastewater under UV-LED controlled illumination.** *Process. Saf. Environ.* **123**, 206–214. <https://doi.org/10.1016/j.psep.2019.01.018>.
- Wu, S., Zhang, L. & Chen, J. 2012 **Paracetamol in the environment and its degradation by microorganisms.** *Appl. Microbiol. Biotechnol.* **96**, 875–884. <https://doi.org/10.1007/s00253-012-4414-4>.
- Xiong, R., Lu, Z., Tang, Q., Huang, X., Ruan, H., Jiang, W., Chen, Y., Liu, Z., Kang, J. & Liu, D. 2020 **UV-LED/chlorine degradation of propranolol in water: degradation pathway and product toxicity.** *Chemosphere* **248**, 125957. <https://doi.org/10.1016/j.chemosphere.2020.125957>.
- Young, B. J., Riera, N. I., Beily, M. E., Bres, P. A., Crespo, D. C. & Ronco, A. E. 2012 **Toxicity of the effluent from an anaerobic bioreactor treating cereal residues on *Lactuca sativa*.** *Ecotoxicol. Environ. Saf.* **76**, 182–186. <https://doi.org/10.1016/j.ecoenv.2011.09.019>.
- Zaidan, L. E. M. C., Pinheiro, R. B., Santana, R. M. R., Charamba, L. V. C., Napoleão, D. C. & Silva, V. L. 2017a **Evaluation of efficiency of advanced oxidative process in degradation of 2-4 dichlorophenol employing UV-C radiation reactor.** *Rev. Eletrônica Gest., Educ. Tecnol. Ambient.* **21**, 147–157. <http://dx.doi.org/10.5902/2236117027766>.
- Zaidan, L. E. M. C., Rodríguez-Díaz, J. M., Napoleão, D. C., Montenegro, M. C. B. S. M., Araújo, A. N., Benachour, M. & Silva, V. L. 2017b **Heterogeneous photocatalytic degradation of phenol and derivatives by (BiPO₄/H₂O₂/UV and TiO₂/H₂O₂/UV) and the evaluation of plant seed toxicity tests.** *Korean J. Chem. Eng.* **34**, 511–522. <https://doi.org/10.1007/s11814-016-0293-1>.
- Zhong, X., Zhang, K.-X., Wu, D., Ye, X.-Y., Huang, W. & Zhou, B.-X. 2020 **Enhanced photocatalytic degradation of levofloxacin by Fe-doped BiOCl nanosheets under LED light irradiation.** *Chem. Eng. J.* **383**, 123148. <https://doi.org/10.1016/j.cej.2019.123148>.